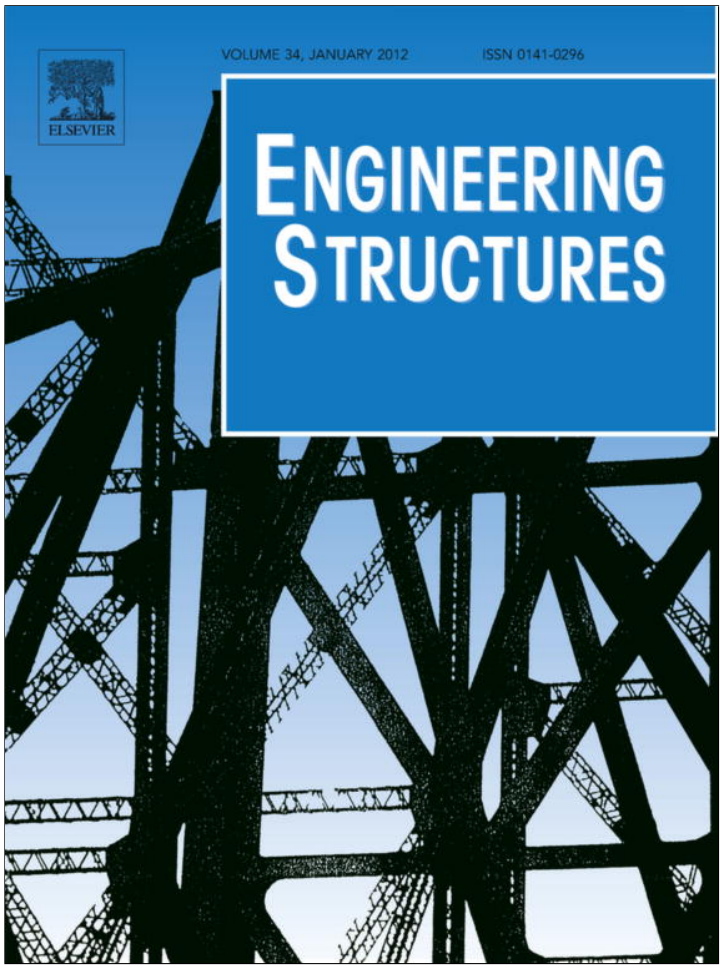

(This is a sample cover image for this issue. The actual cover is not yet available at this time.)

Engineering Structures 39 (2012) 38–49

Contents lists available at SciVerse ScienceDirect

Engineering Structures

journal homepage: www.elsevier.com/locate/engstruct

Skewed concrete box girder bridge static and dynamic testing and analysis

X.H. He [a,*], X.W. Sheng [a], A. Scanlon [b], D.G. Linzell [b], X.D. Yu [a]

[a] School of Civil Engineering, Central South University, Changsha, 410075 Hunan, China
[b] Department of Civil and Environmental Engineering, The Pennsylvania State University, PA, USA

ARTICLE INFO

Article history:
Received 3 March 2011
Revised 20 January 2012
Accepted 30 January 2012

Keywords:
Skew
Concrete
Box girder
Railway
Finite element analysis
Static
Dynamic
Testing

ABSTRACT

Skewed bridges are widely used in China, with one prominent application being for high speed railways, and, as in other parts of the world, certain behavioral aspects need additional research to better understand their performance and to provide additional scientific basis for design. This paper summarizes results of a research project that encompassed 1:8 scale model testing and analyses of a three-span continuous, prestressed concrete (PC), box girder bridge having a 45° skew. The scale-model structure replicates an actual bridge being constructed for a high speed railway between Beijing and Shanghai. Research that is summarized here involved static and dynamic testing. Along with summarizing the design and construction details and the experimental procedure, experimentally obtained displacements and stresses, natural frequencies, mode shapes and damping ratios are presented and compared against those obtained from FE analyses of the tested structures. The influence of skew on the bridge's static and dynamic behavior is also investigated. Research results provide important scientific basis for the design and construction of skewed bridges on high speed railways.

1. Introduction

The continued economic development and increasing investment in infrastructure in China has resulted in a marked improvement in construction standards for transportation networks throughout the country. This investment and development includes the increased design and implementation of high speed rail lines, especially in the more populous eastern portion of the country. Due to geometric and space constraints that can exist in and around high speed rail line construction sites, the superstructure for many bridges on high speed railway lines must be constructed skewed relative to items that the bridge spans to assist with track alignment and avoid undue curvature of the rail line while satisfying high speed demands. The skew angle can be defined as the angle between the normal to the centerline of the bridge and the centerline of the abutment or pier cap [1]. When bridges are not perpendicular to their spanning obstacles two main arrangement styles for the substructure can be used: (1) orthogonal (i.e. ensure the piers and bearings are orthogonal to the longitudinal centerline), which may require longer spans for the bridge, or; (2) skewed (i.e. the piers and bearings are skewed relative to the longitudinal centerline). Skewed bridges are becoming a popular choice for high speed rail bridge designers in China since they can: (a) maintain harmony with the surrounding buildings and environment by requiring less land space for the new structure; (b) reduce resistance to flow for piers located in the water; and (c) meet high speed rail performance demands.

Compared with a bridge having an orthogonal substructure, the behavior of skewed bridges is more complicated due to torsional effects that result from the skew angle. During the past few decades experimental and computational studies of skewed highway bridges have been performed. Scordelis et al. [2] performed a large-scale replica test of a California skewed highway bridge prototype to investigate reactions, deflections, strains and moments. Field testing of skewed concrete bridges was also completed [3–5] along with studies of skewed concrete bridge live load distribution [6,7], seismic analysis [8–11] and dynamic analysis [12,13]. Similar topics for steel and steel–concrete composite skewed bridges have been studied [14–20].

While extensive study of skewed steel and concrete highway bridges has occurred, relatively limited research has focused on skewed railway bridges and especially skewed high speed railway bridges [21–24]. Loading and geometric configurations for high speed railway bridges are significantly different from for highway bridges. The increased static and dynamic live loads induced by a high speed train may result in torsion levels that exceed those found in highway bridges and this, when coupled with reduced widths that railway bridges often have in comparison to highway bridges of similar length, indicates a need for additional research focusing on skewed, railway bridges.

* Corresponding author. Tel.: +86 731 82655012.
E-mail address: xuhuihe@csu.edu.cn (X.H. He).

0141-0296/$ - see front matter © 2012 Elsevier Ltd. All rights reserved.
doi:10.1016/j.engstruct.2012.01.016

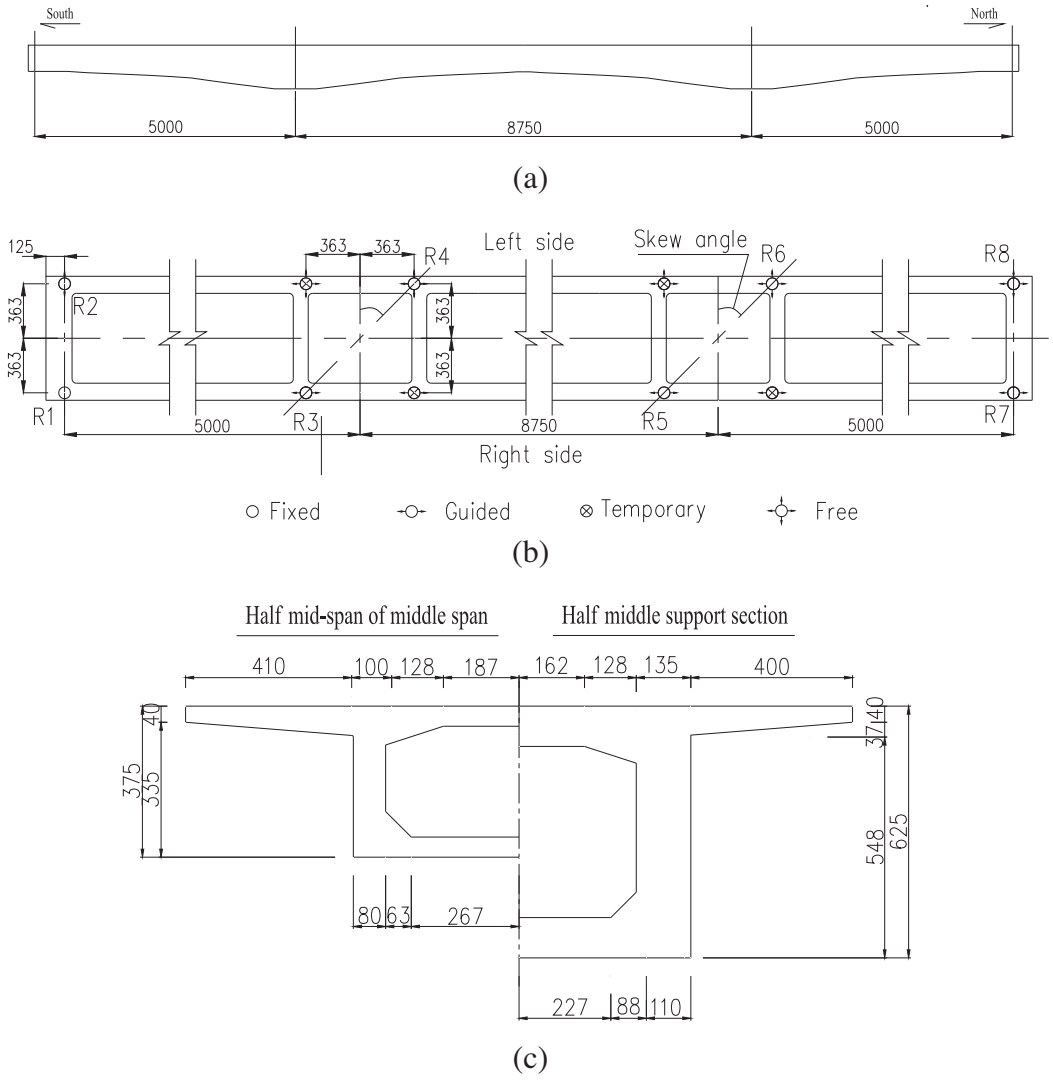

Fig. 1. Model bridge: (a) elevation; (b) framing and support plan; (c) typical cross sections (units: mm).

The Beijing to Shanghai high speed railway is anticipated to be one of the most important high speed railways in China, with design train speeds approaching 350 km/h. The high speed railway is 1318 km long of which 1059 km consists of bridges, approximately 80% of the total length. As a result, bridge behavior and performance is extremely important when assessing the overall performance and success of the railway and the design, testing and examination of the behavior of a representative skewed, concrete bridge was deemed necessary. This led to the design, construction and testing of a 1:8 scale model of a prestressed concrete (PC) box girder bridge with a 45° skew at the Central South University structural testing laboratory. Both static and dynamic testing of the model bridge was completed and this paper summarizes results of these studies. The major objective of the static tests was to examine behavior of skewed structures of small width under dead and live load. Here, small width implies the width to span ratio is smaller than common highway bridges. The major objective of dynamic tests was to establish dynamic properties for these types of structures. Summarized herein are details of the design, construction, instrumentation, testing and analysis of the model bridge. Experimental results for static displacements and stresses along with vibration frequencies, mode shapes and damping ratios of the model bridge are presented and compared with those obtained from computational analyses. In addition, the influences of skew on the bridge's static and dynamic behavior are discussed. This paper focuses on the performance of structures at service load levels for which response remains linearly elastic. Nonlinear response under increasing load is discussed in [25].

2. Model bridge description

One of the bridges to be constructed for the Beijing to Shanghai high speed railway is a three-span, prestressed concrete, skewed box girder bridge having span lengths of 40, 70 and 40 m and a skew angle of 45°. This structure is representative of many skewed bridges found on the railway. A 1:8 scale model of the bridge was constructed and tested in the structures laboratory at Central South University. The model bridge was designed following the laws of similitude, with sections being scaled accordingly and materials being similar to those used for the prototype bridge. Some aspects of the scale model structure had to be modified to facilitate construction, such as having wider box girder webs to accommodate the prestressing strands. The design of unbonded tendons was based on relevant design and technical codes. The overall length of the model bridge was 19 m, consisting of an 8.75 m main span and two side spans of 5 m each. The widths of the model girder flanges were 1.65 m at the top and 0.85 m at the bottom. The bridge depth at mid-span of the center span was

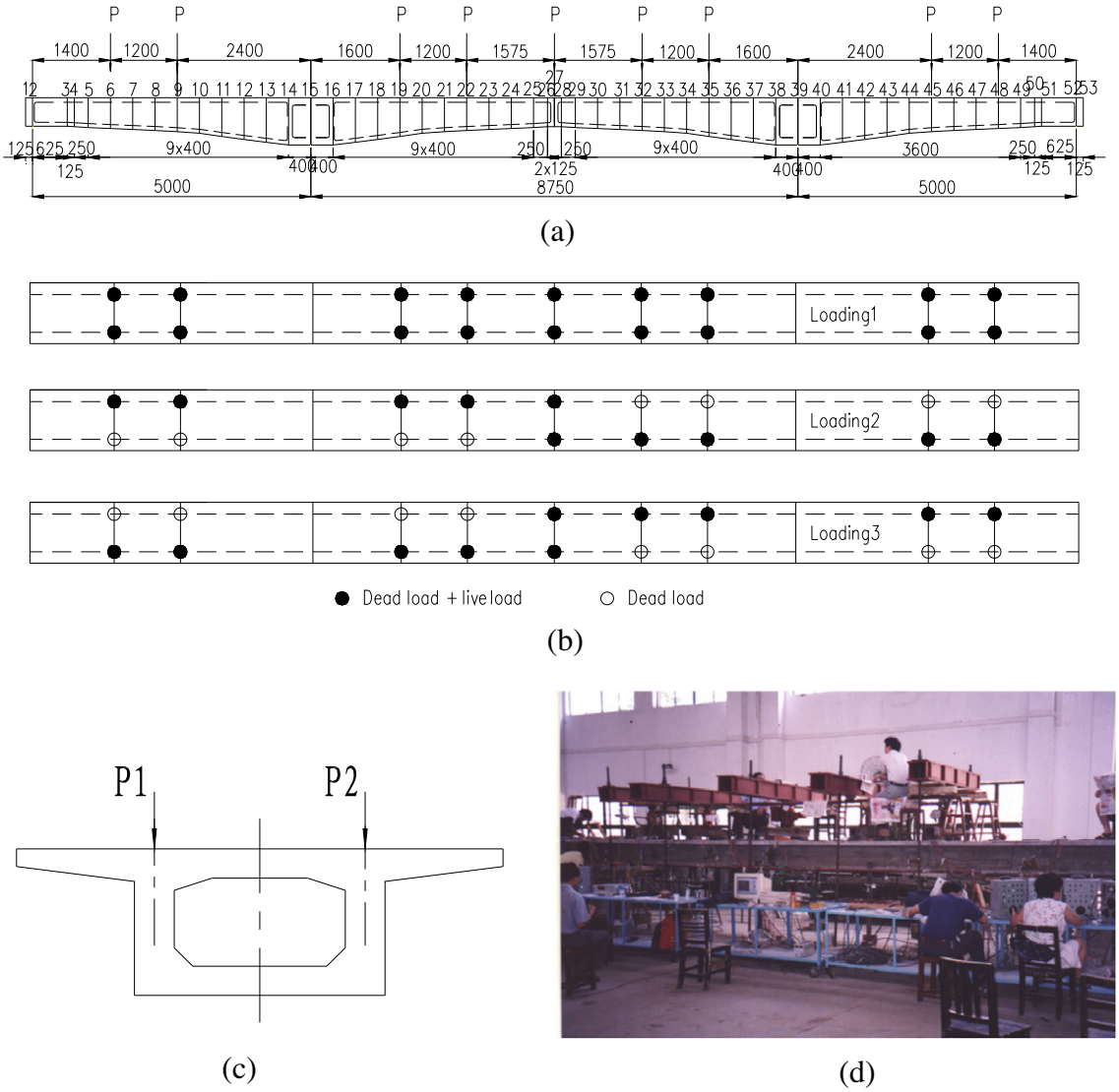

Fig. 2. Model bridge static loading arrangement: (a) loaded sections; (b) plan view; (c) cross section loading; (d) test picture (center span) (units: mm).

Table 1
Static test loading summary (kN).

Loaded sections	Loading 1		Loading 2		Loading 3	
	Left (P1)	Right (P2)	Left (P1)	Right (P2)	Left (P1)	Right (P2)
S6	52.5	52.5	52.5	20	20	52.5
S9	115	115	115	100	100	115
S19	50	50	50	50	50	50
S22	65	65	65	40	40	65
S27	72.5	72.5	72.5	72.5	72.5	72.5
S32	65	65	40	65	65	40
S35	50	50	50	50	50	50
S45	115	115	100	115	115	100
S48	52.5	52.5	20	52.5	52.5	20

0.375 m and at the piers the depth was 0.625 m. The top flange thickness varied between 40 mm and 77 mm, the bottom flange thickness varied between 70 mm and 90 mm and the web thickness was 100 mm except for the support sections. A framing and support plan and typical cross sections are shown in Fig. 1. The model girder bridge was fully prestressed in the longitudinal direction to ensure that the structure was always in compression under the combination of prestressing, dead, and live load. Ten unbonded, continuous prestressed tendons were symmetrically placed across the bridge section. The yield strength of each prestressing strand was 1860 MPa and the prestressing force on each was 181.35 kN. Concrete used for the model bridge was of similar strength to that on the actual structure, with an elastic modulus of 36 GPa and a compressive strength of 50 MPa.

While the actual bridge is constructed segmentally using cantilever construction, the model bridge was cast and prestressed in

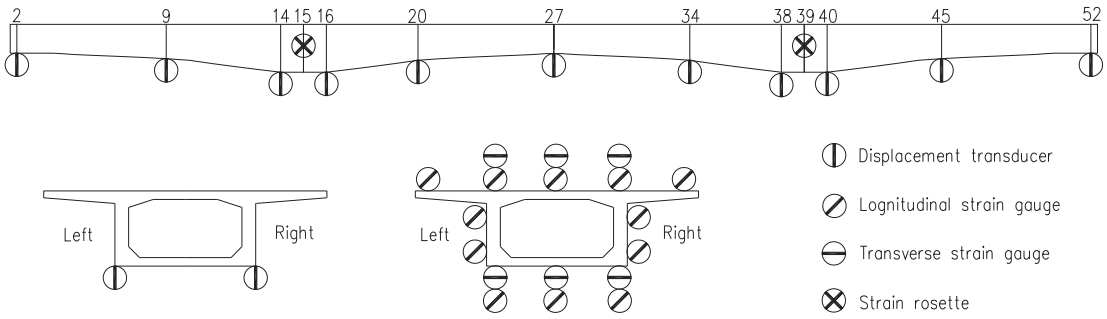

Fig. 3. Displacement transducer and strain gauge locations.

Table 2
Experimental and analytical results for displacements (mm) and twist angles (10^{-4} rad).

Test spans			South side span			Center span			North side span		
Sections number			S9	S14	S16	S20	S27	S34	S38	S40	S45
Loading 1	Left web	FEM	−0.34	0.3	0	−3.1	−5.34	−3.41	−0.56	0	−0.6
		Test	−0.37	0.25	0	−3.39	−5.65	−3.85	−0.83	0	−0.89
	Right web	FEM	−0.6	0	−0.56	−3.41	−5.34	−3.1	0	0.3	−0.34
		Test	−0.56	0	−0.73	−3.7	−5.61	−3.37	0	0.46	−0.61
	Twist angle	FEM	−3.06	−3.53	−6.95	−3.65	0	3.65	6.59	3.53	3.06
		Test	−2.3	−3	−8.56	−3.72	−0.43	5.68	9.76	5.36	3.32
Loading 2	Left web	FEM	−0.28	0.28	0	−2.84	−4.89	−3.1	−0.51	0	−0.46
		Test	−0.75	0.19	0	−2.93	−4.84	−3.1	−0.63	0	−0.52
	Right web	FEM	−0.45	0	−0.51	−3.0	−4.98	−2.84	0	0.28	−0.28
		Test	−0.36	0	−0.53	−3.1	−4.77	−2.8	0	0.38	−0.48
	Twist angle	FEM	−2.06	−3.27	−6.01	−2.97	0	2.97	6.01	3.27	2.12
		Test	–	−2.3	−6.23	−2.03	0.8	3.06	7.39	4.49	0.47
Loading 3	Left web	FEM	−0.11	0.34	0	−2.91	−5.06	−3.27	−0.57	0	−0.45
		Test	–	–	–	–	–	–	–	–	–
	Right web	FEM	−0.45	0	−0.57	−3.27	−5.06	−2.91	0	0.34	−0.11
		Test	–	–	–	–	–	–	–	–	–
	Twist angle	FEM	−3.95	−3.99	−6.65	−4.25	0	5.25	6.65	3.99	3.953
		Test	–	–	–	–	–	–	–	–	–

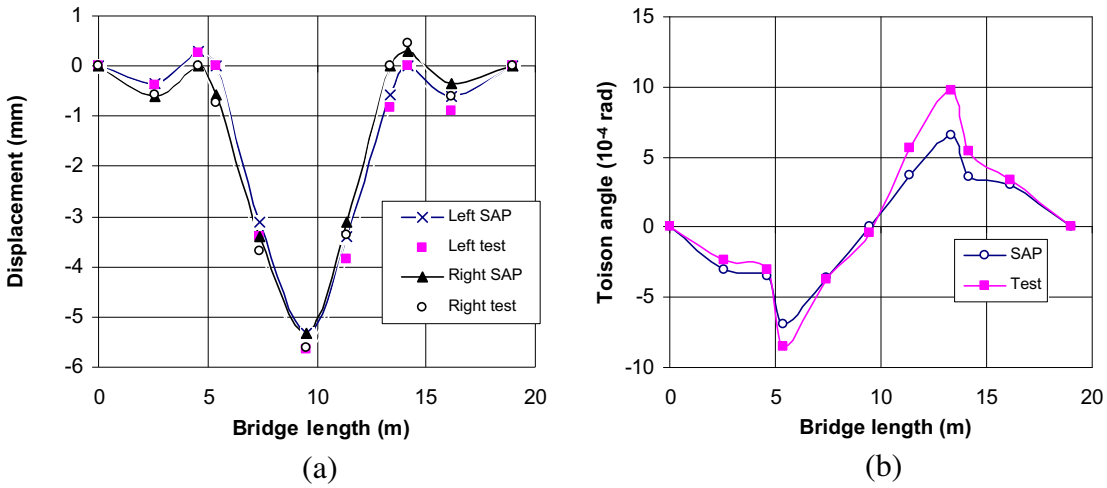

Fig. 4. Loading 1: (a) vertical displacement comparisons; (b) twist angle comparisons.

place using falsework. Initially, the model structure was supported using four bearings on top of the piers for ease of construction. After partial prestressing was completed, two temporary bearings were removed and the structure was transformed to one that was supported by twin bearings skewed at 45° at the piers. In its final, finished state, the model bridge was supported using skewed bearings at the piers to simulate actual support conditions and had similar levels of induced prestressing force to the prototype.

3. Static tests and analyses

3.1. Loading

Static tests of the model bridge were completed to examine and verify behavior under live and dead load. To accurately simulate anticipated maximum loadings on the prototype bridge during the laboratory tests, maximum anticipated stresses of typical

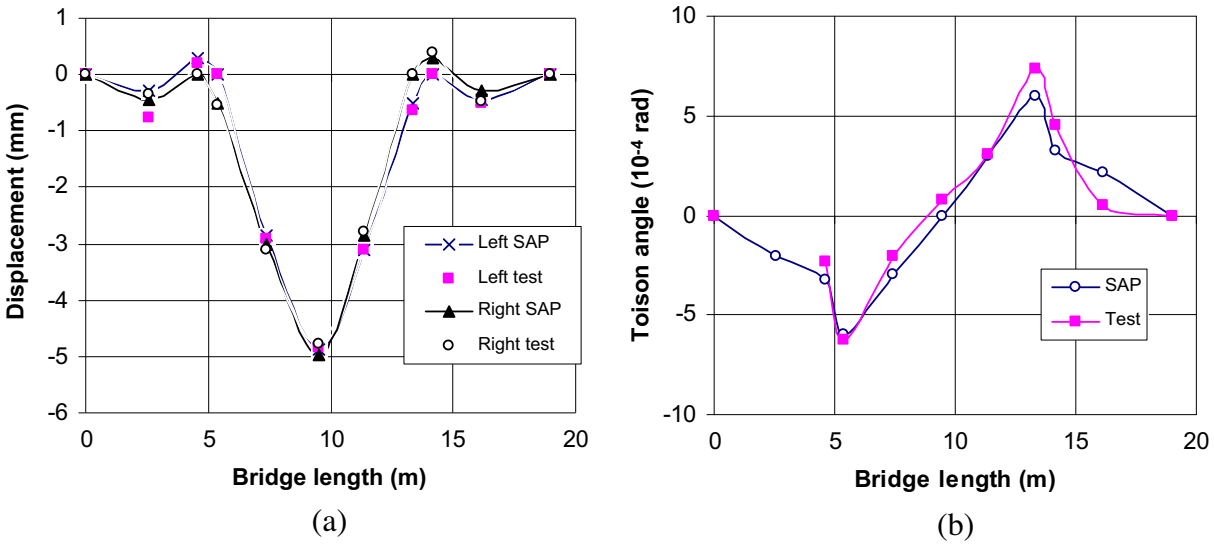

Fig. 5. Loading 2: (a) vertical displacement comparisons; (b) twist angle comparisons.

Table 3
Ratio of normal stresses at web–flange junction to mean web normal stress.

Sections	Loading 1	Loading 2
Web top stress/mean stress		
Pier	1.03–1.11	1.03–1.08
Mid-span of center span	1.00–1.01	1.01
Web bottom stress/mean stress		
Pier	1.10–1.20	1.03–1.07
Mid-span of center span	1.00–1.05	1.03–1.04

Table 4
Box girder extreme fiber normal stress non-uniformity coefficients at typical sections.

Sections	Loading 1	Loading 2
Box girder top flange		
Pier	1.10–1.28	1.06–1.18
Mid-span of center span	1.01–1.20	1.04–1.11
Box girder bottom flange		
Pier	1.10–1.34	1.06–1.21
Mid-span of center span	1.02–1.10	1.03–1.10

Table 5
Web shear stress non-uniformity coefficients.

Positions	Maximum shear stress (MPa)	Non-uniformity coefficient
Left web of pier	−3.540	1.23
Mid-span of center span	−2.012	1.83

sections of the bridge subjected to both self-weight and live loads were calculated. These stresses were determined for a live load case that simulated two side-by-side trains at various locations along the length of the bridge. A total of nine sections were considered along the length: five in the center span and two in each side span (see Fig. 2). Loads were placed onto the bridge section on top of the box webs as shown in Fig. 2. Loading 1 consists of symmetric loading at all loaded sections In addition to Loading 1; two unsymmetric loading conditions were examined to investigate performance under loads that would exacerbate torsion of the box section. The two additional loading conditions examined: (1) dead load plus live loads on the left side of the bridge section shown in Fig. 2b (P1) on the south half of the bridge in plan and on the right side of the section shown in Fig. 2b (P2) on the north half of the bridge in plan (Loading 2); and (2) dead load plus left section live load on the north half of the bridge and right section live load on the south half of the bridge (Loading 3). Load magnitudes and locations for these different conditions are summarized in Table 1. Loading 3 tests were not conducted in the laboratory to avoid anticipated uplift and subsequent safety concerns at select bearing locations, however, analyses were performed for this case and are discussed later.

3.2. Instrumentation

The model box girder was instrumented to record displacements and strains during static testing. Instrumentation consisted of 22 displacement transducers, each having 0.01 mm precision, mounted on the two sides of the box girder webs near the bottom and more than 100 resistance strain gauges measuring concrete and steel reinforcement strains. Static loads were applied using nine jacks and spreader beams as shown in Fig. 2. All instruments were calibrated before installation to minimize instrument and testing system errors. Fig. 3 shows the arrangement of the displacement transducers and strain gauges.

3.3. Finite element model

Static finite element analyses were performed using a 3-dimensional (3D) finite element (FE) model created in SAP [26] that contained both 3D solid and 1D linear elements. Prestressing was modeled using linear elements and those elements were coupled to solid elements representing the concrete via the use of common nodes. Mild steel was not included in the models. Prestressing forces were applied as temperature changes in the prestressed steel strands that produced similar initial stress magnitudes to those measured during construction [27]. The substructure was not explicitly modeled and boundary conditions consisted of roller and pinned supports, with locations and restraint directions matching those for the tested and prototype bridges. Concentrated forces representing train live loads were applied to the model deck nodes following the loading plan (Fig. 2). Prior to studying the

Table 6
Vertical reaction comparisons (kN).

Loading conditions		R1	R2	R3	R4	R	R4/R	(R3 + R4)/R
Loading 1	FEM	60.2	14.9	210.1	352.3	637.5	0.564	0.80
	Test	42.5	23.2	256.2	315.6	637.5	0.495	0.897
Loading 2	FEM	43.5	14.8	164.5	342.2	565.0	0.606	0.897
	Test	40.5	7.2	205.3	312.0	565.0	0.552	0.916
Loading 3	FEM	68.4	−13.0	189.2	320.5	565	0.567	0.902

Table 7
Influence of skew angle on behavior.

Skew angles (°)	Reactions (kN)				Moments (kN m)		T/S27 (kN m)	D/S27 (mm)	TA/S14 (10^{-4} rad)
	R1	R2	R3	R4	S15	S27			
0	33.4	33.4	285.4	285.4	−638.2	261.9	0	5.81	0
10	40.7	26.4	269.2	301.3	−617.5	261.5	6.96	5.79	1.32
20	47.7	20.4	252.5	316.9	−594.4	260.1	14.02	5.73	2.64
30	53.9	16.1	235.4	332.1	−566.7	257.4	20.97	5.61	3.96
40	58.6	14.4	218.3	346.1	−531.8	253.3	27.82	5.44	5.24
45	60.2	14.9	210.1	352.3	−510.2	250.5	30.92	5.34	5.83
50	61.2	16.4	202.6	357.3	−484.5	247.1	33.60	5.19	6.35
60	61.1	22.9	192.0	361.5	−414.1	238.2	36.81	4.82	6.95

effects of skew on static response, the FE model was calibrated by comparing maximum predicted and measured vertical deformations and stresses for Loading 1. Detailed calibration information and results are reported in [28].

3.4. Deformations

To demonstrate the effects of skew on a narrow, railway structure and to show some typical calibration comparisons, selected computational and measured vertical displacements and twist angles under static loading conditions are compared in Table 2 and Figs. 4 and 5. As seen in the table and figures, good agreement between computational and experimental results for vertical displacements and twist angles under all three loading conditions was obtained. In addition, for symmetric Loading 1, it was observed that displacement of the two box girder webs was anti-symmetric except at the support locations and at mid-span of the center span, where an inflection point existed. For unsymmetric Loading 2, vertical displacements and twist angles were again anti-symmetric with smaller twist angles and vertical displacements when compared to Loading 1. For unsymmetric Loading 3, computational results indicated that twist angles were anti-symmetric with slightly larger angles existing when compared to Loading 1 and 2. Therefore, it was concluded that, for the loading cases that were examined, torsional deformations of skewed box girder bridge would be controlled by Loading 3.

3.5. Normal stresses

Experimental and computational normal stresses for the model bridge indicated that the structure was still in the elastic range during the static tests. However, non-symmetrical normal stresses were observed, indicative of warping, shear lag and transverse bending effects due to the skew. Ratios of maximum normal stresses at the top and bottom of the webs to the mean web normal stress values are listed in Table 3. For Loading 2, there was no torsion effect at mid-span of the center span where the torsion inflection point existed.

The level of torsion in the box girder section was also examined via calculation of non-uniformity coefficients, C, using the following formula:

$$C = \frac{\sigma_m}{\bar{\sigma}} \tag{1}$$

where σ_m is the maximum stress value and σ the mean stress value, both of which are measured at the extreme fibers of the flanges. Resulting coefficients, found for both the top and bottom flanges, are listed in Table 4. The table indicates that the loading conditions that were examined all induced torsion in the box section and it also shows that the unsymmetric load condition (Loading 2) induced lower torsional stresses than the symmetric loading condition (Loading 1). In addition, the twist effects are smaller in the center span and over the piers than for the side spans.

3.6. Web shear stresses

Levels of shear stress in the box girder webs were examined for Loading 1, the symmetrical condition, and non-uniformity coefficients, found using an equation for shear stress similar to Eq. (1), were again used. Resulting coefficients are listed in Table 5. Non-uniformity coefficients for the left web at the pier and at mid-span of the center span sections are 1.23 and 1.83, respectively, values which again indicate appreciable torsion in the bridge due to skew.

3.7. Vertical reactions

Experimental and computed vertical reactions under different loading conditions are listed in Table 6. As seen in the table, both experimental and computational results show that the two reactions at each pier (R3, R4) are not equal but do indicate higher reactions at the obtuse corner of the structure when viewed in plan compared to those at the acute corner. In addition, under Loading 3, bearing R2 shows uplift, a clear indicator of skew influence on live load distribution. Therefore, for narrow, skewed, box girder bridges, similar to the double-line railway bridges that were examined here, designers should consider using multiple moving loads, with those loads heading in opposite directions, simultaneously to adequately account for possible bearing uplift.

3.8. Influence of skew angle on behavior

In order to investigate the elastic performance of narrow, skewed box girder bridges, such as those used for high speed rail,

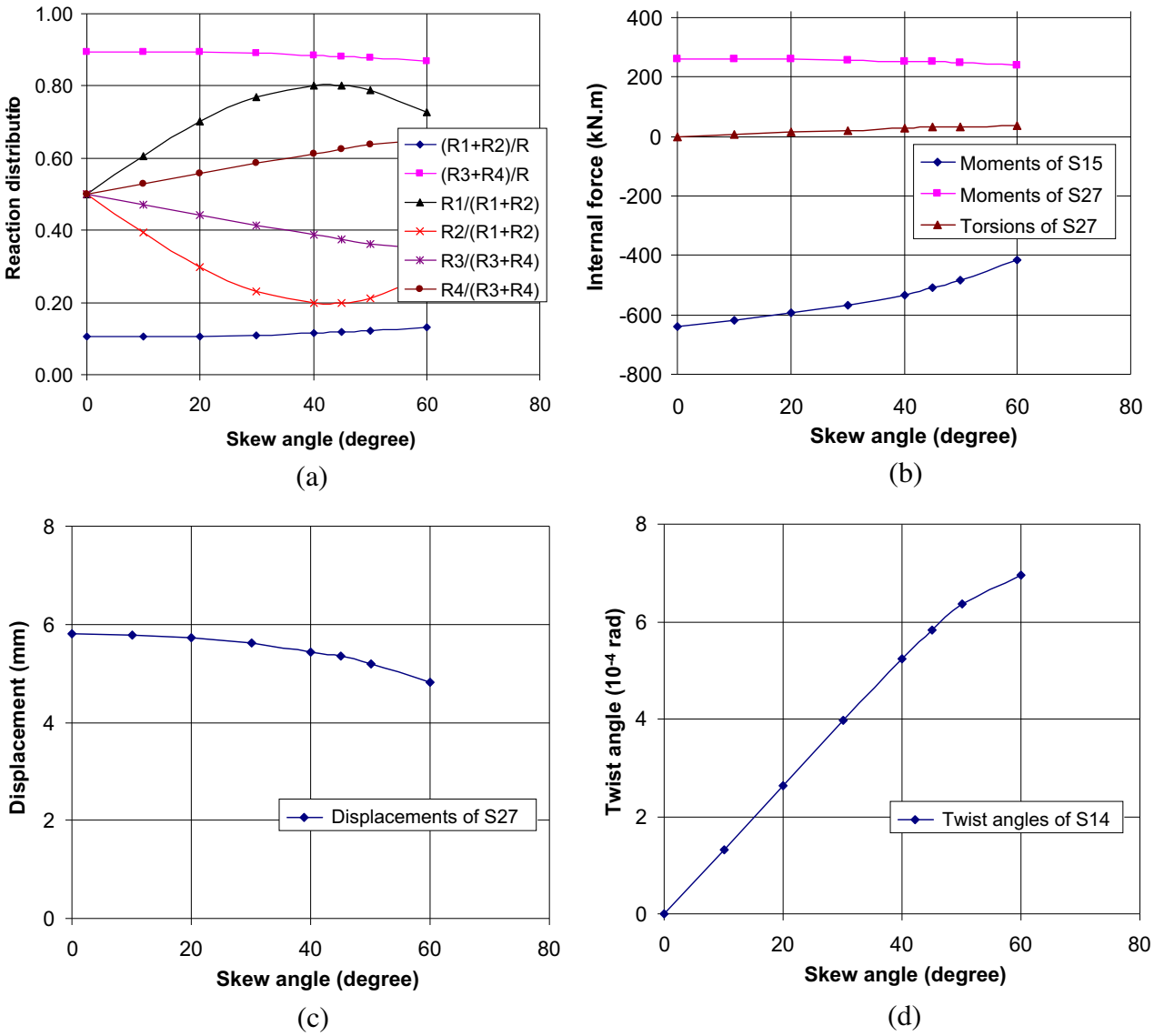

Fig. 6. Influence of skew angle on behavior: (a) reactions; (b) bending moments and torsion; (c) displacements; (d) twist angles.

Table 8
Influence of width to span ratio (B/L) on behavior.

B/L	Reactions (kN)				Moments (kN m)		T/S27 (kN m)	D/S27 (mm)	TA/S14 (10^{-4} rad)
	R1	R2	R3	R4	S15	S27			
0.04	43.9	25.9	255.7	312.0	−520.45	256.05	12.20	8.82	10.60
0.06	51.5	20.8	234.7	330.5	−515.53	253.70	20.76	7.06	8.16
0.08	56.7	17.3	219.9	343.6	−512.10	251.88	26.86	6.30	6.70
0.0943	60.2	14.9	210.1	352.3	−510.20	250.50	30.92	5.34	5.83
0.10	60.7	14.5	208.7	353.6	−509.86	250.17	31.46	5.24	5.71
0.12	63.9	12.3	199.7	361.1	−508.25	248.67	35.20	4.70	5.00
0.14	66.5	10.5	192.2	368.3	−507.07	247.17	38.31	4.27	4.46
0.16	68.7	8.9	185.8	374.0	−506.22	245.78	40.98	3.95	4.03

as a function of the angle of skew bridge deformations and reactions were studied computationally. These FE models were created based on the calibrated 1:8 scale bridge FE models, with only the skew angle being varied. The studies examined the effects of skew angles between 0° and 60° on resulting reactions, moments, torsions (T), vertical displacements (D) and twist angles (TA). Results under Loading 1 are shown in Table 7 and in Fig. 6 for sections S15 and S27, which represent bridge sections over the pier and at mid-span of the center span, respectively (see Fig. 1). They can be summarized as follows:

- An increase of skew angle increases abutment reactions (R1 + R2) slightly but reduces pier reactions (R3 + R4).
- Increasing skew can reduce the negative moments over the pier section (S15) and the moments and displacements at mid-span of the center span section (S27).

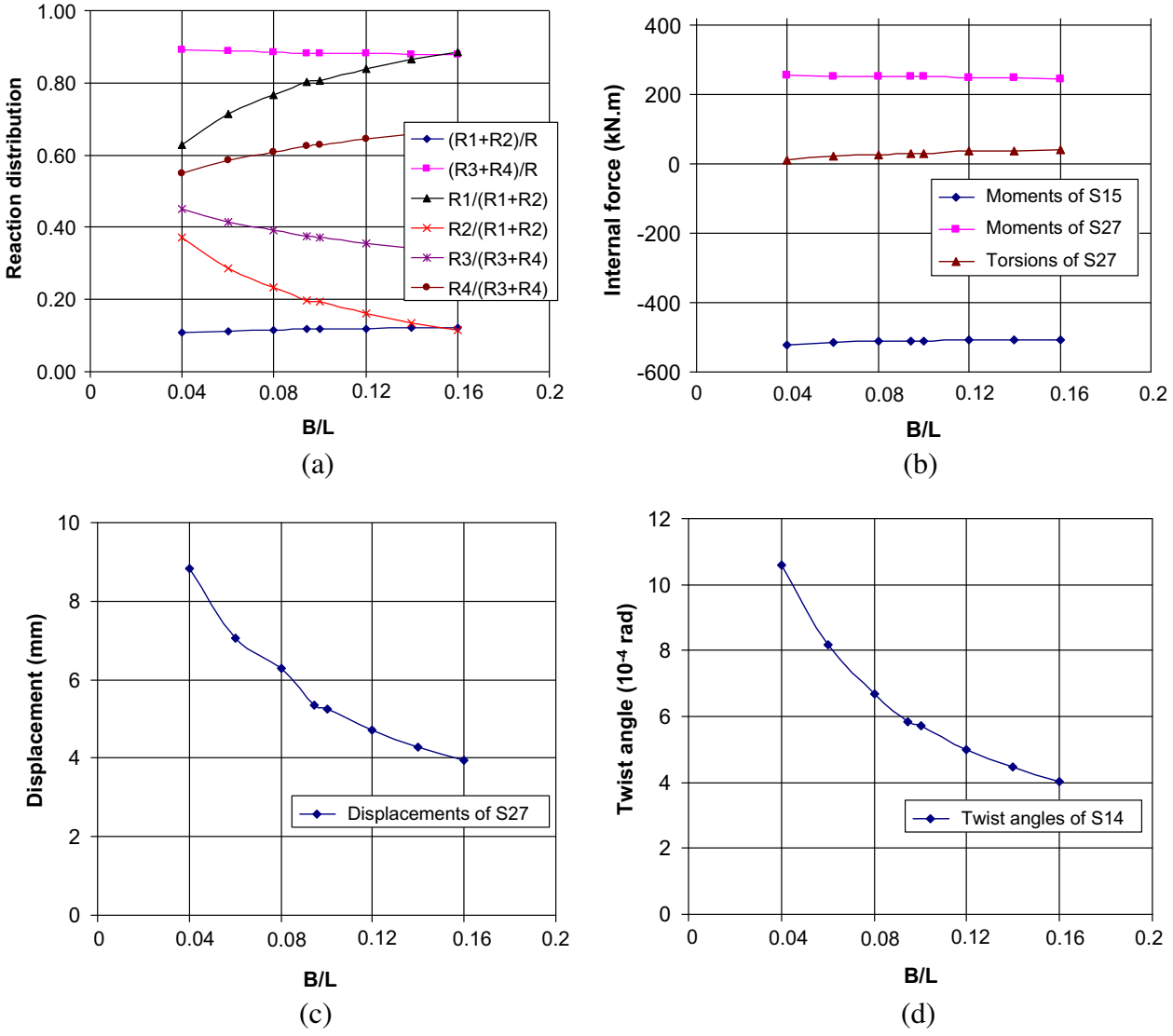

Fig. 7. Influence of width to span ratio (B/L) on behavior: (a) reactions; (2) bending moments and torsion; (c) displacements (d) twist angles.

- Increasing skew increases torsion effects and, for skew angles between 40° and 60°, torsion effects at mid-span of the center span approach 10–15% of the corresponding vertical bending moments.
- The effects of skew on the structure appear to change markedly once the skew angles exceed 45°. Consequently, large skew angles were not recommended for bridges on the Beijing to Shanghai high speed railway.

3.9. Influence of relative bending to torsional stiffness on behavior

Another important factor shown to influence the effect of skew on bridge behavior is the bending (EI) to torsional stiffness (GJ) ratio [16,29]. For a box girder bridge, this ratio can be simplified to a ratio of the structure's width (B) to span (L) when it assumed that the bridges being compared have similar spans, skew angles, support conditions, girder depths and flange thicknesses To facilitate these types of comparisons for the current study, it was assumed that the box girder bottom flange width varied while the top flange width remained constant. For a 45° skew angle under symmetric Loading 1, results that examined the influence of width to span ratio (B/L) on various quantities are summarized for sections S15 and

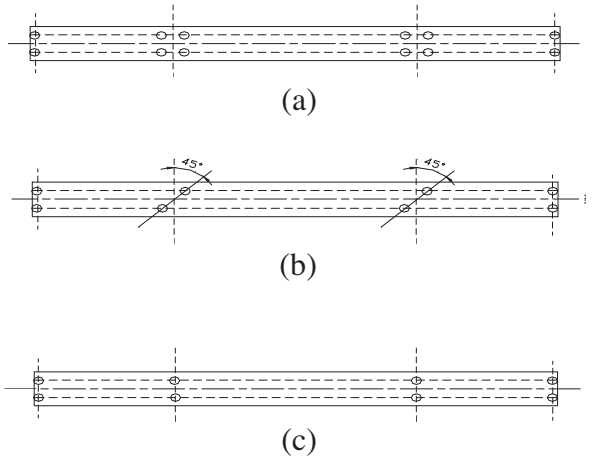

Fig. 8. Different bearing arrangements: (a) orthogonal double bearing; (b) skewed bearing; (c) orthogonal single bearing.

S27 in Table 8 and in Fig. 7. The results indicate that the B/L ratio had appreciable influence on box girder bridge reactions, torsion

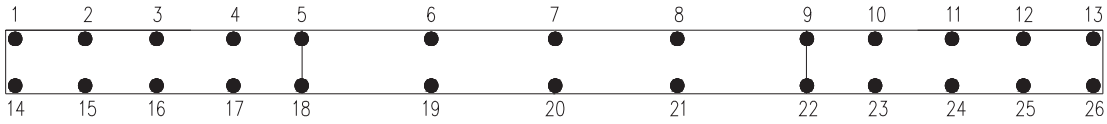

Fig. 9. Dynamic measurement locations.

Table 9
Dynamic characteristic comparisons.

Mode no.	Orthogonal double bearing			Skewed bearing (45°)			Orthogonal single bearing	
	Frequencies (Hz)		Modes nature	Frequencies (Hz)		Modes nature	Frequencies (FEM, Hz)	Modes nature
	FEM	Test		FEM	Test			
1	28.91	29.38	VSF	20.66	20.46	VSF	19.01	VSF
2	30.04	31.89	VAF	31.51	32.53	VAF–T	32.77	SVF
3	44.33	43.44	TF	35.56	34.33	T–TF–SVF	34.91	TF
4	55.29	56.13	STF	42.94	41.21	T–TF–SVF	42.11	VAF
5	60.84	–	STF	53.61	54.56	VSF–T	53.25	VSF
6	66.25	–	T–STF	58.88	–	T–TF	56.75	T–STF
7	69.17	–	VAF–T	68.40	–	STF–SVF–T	61.03	T–STF

Note: vertical symmetric flexure, VSF; vertical anti-symmetric flexure, VAF; torsion, T; transverse flexure, TF; side span vertical flexure, SVF; side span transverse flexure, STF.

(T) levels, vertical displacements (D) and twist angles (TA), but less influence on bending moments. In addition, increasing or decreasing the width can lead to impractical structures even if the effects are beneficial, and the chosen design B/L (0.0943) for the prototype appears to be a good compromise between practicality and structural efficiency.

4. Dynamic tests and analyses

4.1. Ambient vibration testing

Ambient vibration testing of the model bridge was completed to measure its dynamic characteristics [30]. The random decrement technique method [31] was used for modal extraction and identification. The dynamic tests included two phases; the first being completed with the bridge under the initial, non-skewed support system described earlier, i.e. the orthogonal double bearing support system shown in Fig. 8a. The second was carried out after the structure was supported by the final, skewed, bearing system, i.e. the two temporary bearings on the top of the two middle piers were dismantled and the orthogonal double bearing system was converted to the skewed bearing system as shown in Fig. 8b. An additional computational examination of a third, non-skewed support system was also completed as shown in Fig. 8c.

4.2. Instrumentation

There were a total of 26 dynamic measurement locations on the both sides of the bridge deck. These locations were near the supports and at mid-span and the ¼ points of the center span as shown in Fig. 9. To identify the vertical and lateral mode shapes of the bridge, each measurement location included a vertical and lateral accelerometer. The sampling frequency was 200 Hz and the sampling time was 30 min.

4.3. Finite element models

Dynamic finite element analyses were carried out using a FE model that contained solid elements to represent the box girder. The prestressing was modeled following the procedures used for the static models and similar boundary conditions were applied. In similar fashion to the static models, the dynamic FE model was calibrated by comparing predicted and measured modal characteristics [32].

4.4. Frequencies and mode shapes

Measured and calculated frequencies and mode shapes for the different bearing conditions are compared in Table 9 and shown in Fig. 10. It should be noted that higher modal frequencies could not be obtained because of difficulty associated with exciting higher modes during ambient vibration testing. In the table, VSF represents vertical symmetric flexure, VAF represents vertical anti-symmetric flexure, T represents torsion, TF represents transverse flexure, SVF represents side span vertical flexure, and STF represents side span transverse flexure. In addition, to investigate the influence of skew angle on railway bridge dynamic behavior, natural frequencies for skew angles from 0° to 60° were obtained and are listed in Table 10 and shown in Fig. 11. Examination of the results indicated the following:

- Good agreement exists between computational and experimental results for the lower modal frequencies and mode shapes.
- The three different bearing conditions had a similar first mode shape (VSF) but differing higher mode shapes. The torsion (T) mode occurred as early as the second mode for the skewed structure, but not until the sixth mode for the orthogonally supported bridges. This indicates that skew can advance the prevalence of torsion during a dynamic event but, for a structure that is narrow relative to its length, flexure appears to be the predominant mode irrespective of skew. This trend also typically occurred with the combined modes, including transverse flexure (TF), side span vertical flexure (SVF), side span transverse flexure (STF), vertical symmetric flexure (VSF) and vertical anti-symmetric flexure (VAF).
- Different support conditions and skews had minimal effect on the first mode shape of the model bridge. Increasing skew was observed to increase the first modal frequency, but no obvious trend for the higher modes was observed. As a result of these findings, it appears that skew increases the apparent stiffness relative to mass.

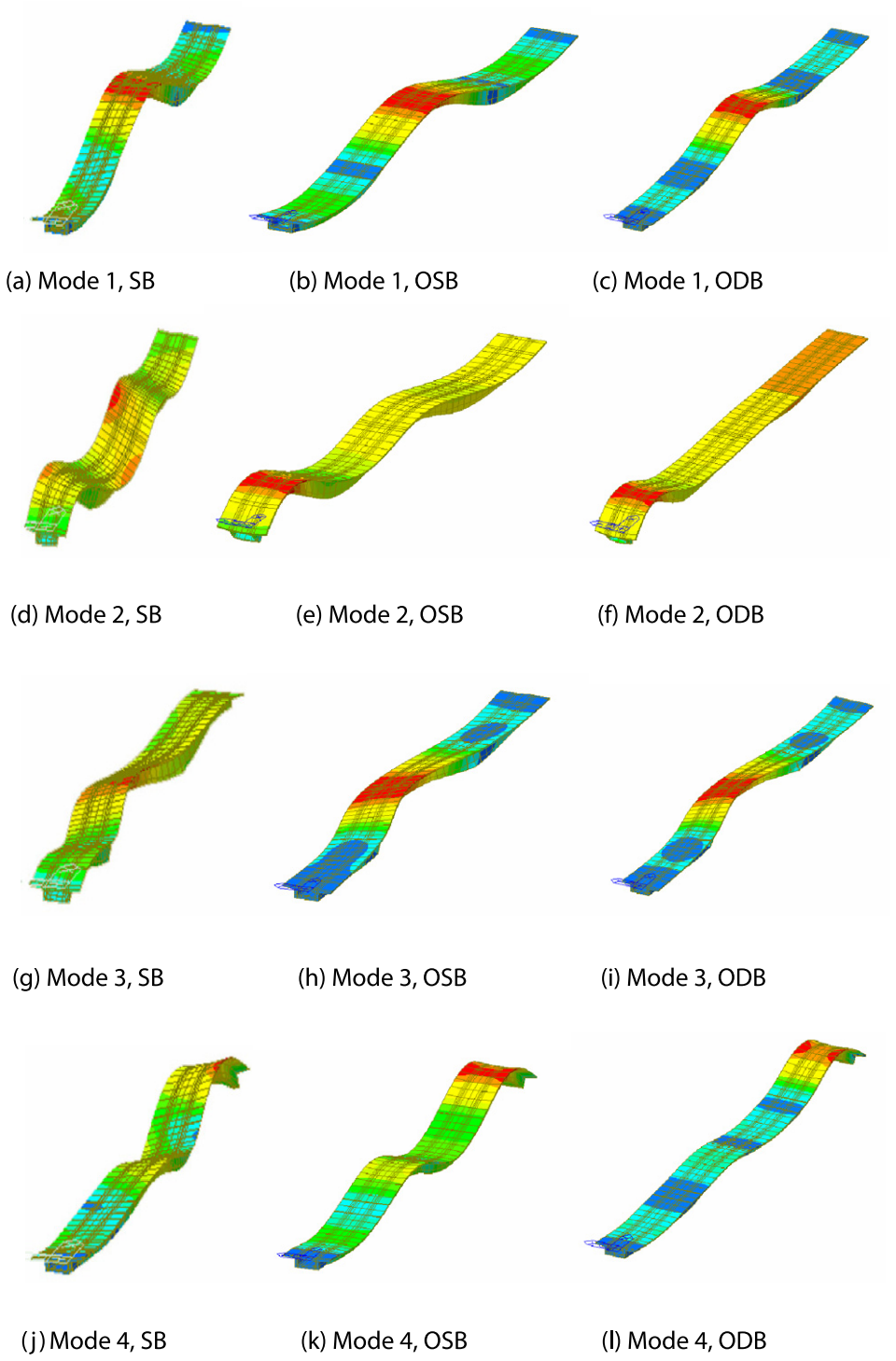

Fig. 10. Calculated mode shapes comparison of skewed bearing (SB), orthogonal single bearing (OSB) and orthogonal double bearing (ODB) bridges.

4.5. Modal damping ratio

Using the RDT method, the first several modal damping ratios for the different support condition model bridges were identified. The measurements of the first three modal damping ratios for the skewed bridge were 1.61%, 1.56% and 1.32%, respectively, which are slightly smaller than those of the orthogonal bearing bridge (1.98%, 1.83% and 1.47%, respectively). It is apparent that, for higher modes, the effects of modal damping decrease as skew increases. However, these effects are small when compared to straight bridges and the effects of skew on modal damping need not be considered. It should be noted that explicitly identifying factors that influence the modal damping ratio outside of the variation in skew, factors that can include material damping, ambient media to vibration damping, and damping caused by the bearing supports and other items, can be quite difficult. Therefore, the authors chose to strictly compare differences between modal damping ratios as a function of skew.

Table 10
Influence of skew angle on natural frequencies.

Skew angles (°)	Modal frequencies (Hz)						
	1	2	3	4	5	6	7
0	19.01	32.77	34.91	42.11	53.25	56.75	61.03
10	19.12	32.79	36.50	42.27	53.95	60.38	66.30
20	19.30	32.65	36.21	42.39	53.87	59.62	66.58
30	19.64	32.38	35.92	42.59	53.77	59.06	67.08
40	20.23	31.88	35.64	42.82	53.65	58.75	67.80
45	20.66	31.51	35.56	42.94	53.61	58.88	68.40
50	21.27	31.01	35.47	43.04	53.63	59.15	69.17
60	23.17	29.46	35.36	42.95	53.64	60.08	71.11

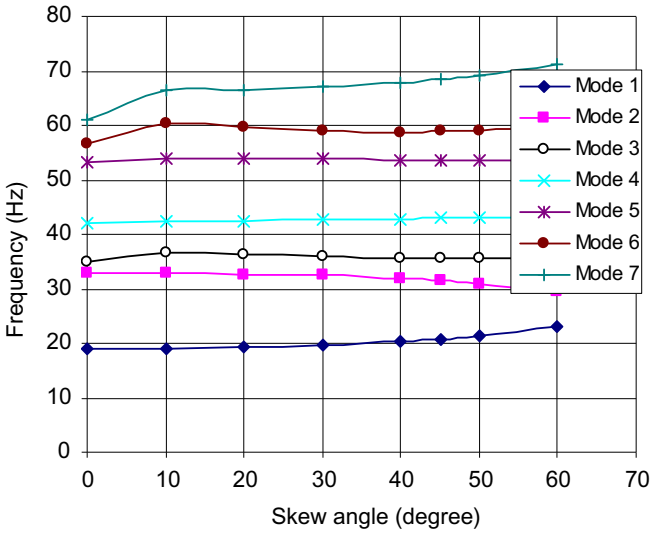

Fig. 11. Influence of skew angle on natural frequencies.

5. Conclusions

Concrete box girders are commonly used for railway bridges in China due to their high strength to weight ratio and enhanced torsional resistance. However, local site conditions may render the use of an orthogonally supported structure not feasible and a skewed structure may be needed. There has been relatively little research related to the performance of skewed bridges in general and especially skewed railway bridges in particular. In this paper, static and dynamic testing and corresponding FE analyses of a three-span, 1:8 scale, continuous, skewed, concrete, box girder bridge that matches a bridge under construction on the Beijing to Shanghai high speed railway are summarized. Based on the analysis and experimental results, it can be concluded that:

(1) Good agreement was obtained between finite element modeling and test results for both static and dynamic loading.
(2) Static Loading 3, an anti-symmetric live loading case, was determined to be a critical design loading arrangement for the box girder bridges on the railway due to the possibility of bearing uplift. Therefore, it is apparent that for narrow box girder bridges of similar geometry to the case examined here, design should be completed considering multiple arrangements of train loading to accurately account for skew effects and any possible bearing uplift that may occur.
(3) For box girder bridges having similar spans and bearing conditions, a higher width to span ratio (B/L) reduces the vertical displacement and torsional deformations but increases the torsional stresses in the structure. Vertical bending moments are slightly affected. In addition, increasing or decreasing box girder width can result in impractical structures even if the effects are beneficial. It appeared that the selected B/L value for the prototype was a good compromise between practicality and structural efficiency.
(4) As box girder bridge skew angles increase, vertical bending moments and deformations decrease. However, torsional stresses and deformations increase as well as differential reaction levels. Consequently, large skew angles (above 45°) were not recommended for skewed bridges on the high speed railway.
(5) Increasing skew was observed to increase the first modal frequency for box girder bridges, but no obvious trend for the higher modes was observed. As a result of these findings, it appears that skew increases the apparent stiffness relative to mass.
(6) Both test and computational results show that torsional modes occurred as early as the second mode for skewed box girder structures, but not until the sixth or higher modes for orthogonally supported box girder bridges. This indicates that skew can advance the prevalence of torsion during a dynamic event but, for a structure that is narrow relative to its length, flexure appears to be the predominant mode irrespective of skew.
(7) Skewed box girder bridge higher mode damping ratios were smaller than those for lower modes and all damping ratios were slightly smaller than those for similar modes for a bridge with no skew. Though damping effects are slightly lessened when skew exists, the effects of skew on damping were shown to be negligible.

Acknowledgements

The work described in this paper was supported in part by a grant from the National Natural Science Foundations of China (Project Nos. 51178471 and 50808175) and partially by a grant from the Ministry of Railways, China (Project No. 98D02).

References

[1] Menassa C, Mabscout M, Tarhini K, Frederick G. Influence of skew angle on reinforced concrete slab bridges. J Bridge Eng 2007;12(2):205–14.
[2] Scordelis AC, Wasti ST, Seible F. Structural response of skew RC box girder bridge. J Struct Eng 1982;108(1):89–104.
[3] Aref AJ, Alampalli S, He YH. Performance of a fiber reinforced polymer web core skew bridge superstructure – Part I: Field testing and finite element simulations. Compos Struct 2005;69:491–9.
[4] Ashebo DB, Chan THT, Yu L. Evaluation of dynamic loads on a skew box girder continuous bridge – Part I: Field test and modal analysis. Eng Struct 2007;29(6):1052–63.
[5] Ashebo DB, Chan THT, Yu L. Evaluation of dynamic loads on a skew box girder continuous bridge – Part II: Parametric study and dynamic load factor. Eng Struct 2007;29(6):1064–73.
[6] Barr PJ, Eberhard MO, Stanton JF. Live-load distribution factors in prestressed concrete girder bridges. J Bridge Eng 2001;6(5):298–308.
[7] Khaloo AR, Mirzabozorg H. Load distribution factors in simply supported skew bridges. J Bridge Eng 2003;8(4):241–4.
[8] Meng JY, Lui EM. Seismic analysis and assessment of a skew highway bridge. Eng Struct 2000;22:1433–52.
[9] Sevgili G, Cancer A. Improved seismic response of multisimple-span skewed bridges retrofitted with link slabs. J Bridge Eng 2009;14(6):452–9.
[10] Maleki S. Deck modeling for seismic analysis of skewed slab-girder bridges. Eng Struct 2002;24(10):1315–26.
[11] Dimitrakopoulos EG. Seismic response analysis of skew bridges with pounding deck–abutment joints. Eng Struct 2011;33(3):813–26.
[12] Wyss JC, Su D, Fujino Y. Prediction of vehicle-induced local responses and application to a skewed girder bridge. Eng Struct 2011;33(4):1088–97.
[13] Kalantari A, Amjadian M. An approximate method for dynamic analysis of skewed highway bridges with continuous rigid deck. Eng Struct 2010;32(9):2850–60.
[14] Battistini A, Quandrato C, Helwig T, Engelhardt M, Frank K. Effectiveness of bent plate connection for end cross-frames in skewed steel bridges. In: Proc

struct congr – don't mess struct eng: expanding role, ASCE, Austin, TX, USA; 2009. p. 11–20.
[15] Choo T, Linzell D, Lee J, Swanson J. Response of a continuous, skewed, high performance steel, semi-integral abutment bridge during deck placement. J Constr Steel Res 2007;61(5):567–86.
[16] Ebeido T, Kennedy JB. Girder moment in continuous skew composite bridges. J Bridge Eng 1996;1(1):37–45.
[17] Meng JY, Ghasemi H, Lui EM. Analytical and experimental study of a skew bridge model. Eng Struct 2004;26(8):1027–142.
[18] Norton EK, Linzell DG, Laman JA. Examination of the response of a skewed steel bridge superstructure during deck placement. Transport Res Rec J Transport Res Board 2003;1845:66–75.
[19] Saiidi M, Randall M, Maraqakis E, Isakovic T. Seismic restrainer design methods for simply supported bridges. J Bridge Eng 2001;6(5):307–15.
[20] Smith DA, Hendy CK. Strengthening of Irwell Valley Bridge, UK. Proc Inst Civ Eng Bridge Eng 2008;161(1):33–43.
[21] Kaliyaperumal G, Imam B, Righiniotis T. Advanced dynamic finite element analysis of a skew steel railway bridge. Eng Struct 2011;33(1):181–90.
[22] Brencich A, Gambarotta L. Assessment procedure and rehabilitation of riveted railway girders: The Campasso Bridge. Eng Struct 2009;31(1):224–39.
[23] Hoelke A. Vibration tests on prestressed concrete railway bridge. Int Ry Congr Assn – Mon Bul 2009;42(8–9):589–600.
[24] Matsumoto Y. Study on reinforced concrete skew girder for railway bridges. Tokyo. Y Tech Res Inst – Quart Rep 1966;7(2):17–9.
[25] Sheng XW, Xin XZ. Nonlinear analysis of the prestressed concrete skew box continuous girder. Zhongguo Tiedao Kexue 2005;26(2):64–8.
[26] Beijing Civil King Software Technology Co., Ltd. Chinese version user manual of SAP2000. Beijing: China Communications Press; 2006.
[27] Zhang SR, Zhu Q, Li S. Simulation methods of prestress in numerical analysis of large aqueduct. Shuili Fadian Xuebao 2009;28(3):97–100+90.
[28] Sheng XW. Theoretical analysis and test study of prestressed concrete skew box girder bridge. Ph.D. thesis. Changsha: Central South University; 2001.
[29] Khaleel MA, Itani RY. Live-load moment for continuous skew bridge. J Struct Eng 1990;116(9):2361–73.
[30] Ren WX, Harik IE, Blandford GE, Lenett M, Baseheart TM. Roebling suspension bridge: II – Ambient testing and live-load response. J Bridge Eng 2004;9(2):119–26.
[31] He XH, Hua XG, Chen ZQ, Huang FL. EMD-based random decrement technique for modal parameter identification of an existing railway bridge. Eng Struct 2011;33(4):1348–56.
[32] He XH, Sheng XW, Chen ZQ. Model test study of vibration characteristics on PC skew box girder bridge of civil high speed rail way. Tiedao Xuebao 2002;24(5):89–92.